J Mater Sci (2011) 46:5332–5344
DOI 10.1007/s10853-011-5471-2

Characterisation of two chemical compounds formed between hydrated portland cement and benzene-1,2-diol (pyrocatechol)

Thomas D. Dyer

Received: 12 January 2011 / Accepted: 14 March 2011 / Published online: 31 March 2011

Abstract Exposure to benzene-1,2-diol (pyrocatechol), a common soil contaminant, has been shown to cause loss of strength in concrete. Synthesis and characterisation of two compounds formed when Portland cement comes in contact with benzene-1,2-diol has been conducted. These compounds are (benzene-1,2-diolato(1-))hydroxidocalcium(II) (formula: $[Ca(C_6O_2H_5)OH]$) and triaqua(benzene-1,2-diol)(benzene-1,2-diolato(1-))hydroxidocalcium(II) (formula: $[Ca(C_6O_2H_5)(C_6O_2H_6)(H_2O)_3(OH)]$). The compounds may play a role in the deterioration process. Characterisation was conducted in terms of thermal decomposition behaviour, infra-red spectra and crystal structure (using powder X-ray diffraction). The likely thermal decomposition reactions of both compounds have been determined, and features in the infra-red spectra assigned to molecular vibrations. Both structures have been solved, with the exception of the location of some hydrogen atoms, and the structures refined using Rietveld refinement methods. It is anticipated that both the thermal analysis data obtained, and crystal structures deduced, in this article can now be used to quantify these phases in cement and concrete exposed to benzene-1,2-diol.

Introduction

During investigations into the interaction of soils contaminated with phenolic compounds and Portland cement, two compounds have been observed to form simultaneously.

Crystals of the compounds are formed when cement paste surfaces are brought into contact with solutions of benzene-1,2-diol (pyrocatechol, $C_6H_6O_2$). Benzene-1,2-diol can be present in many soils as a result of contamination from the industrial processing of fossil fuels or as a result of natural biological processes. Figure 1 is a powder X-ray diffraction trace obtained from a slice taken from the surface of a Portland cement paste exposed immediately after mixing to a solution containing benzene-1,2-diol. The presence of the two compounds is indicated on this plot, with the most prominent diffraction peak for the first—Compound 1—occurring at around 7.2°2θ, and 13.0°2θ for Compound 2. These compounds were confirmed as separate entities by the fact that the intensities of their patterns changed independently at different exposure concentrations.

Exposure to many phenolic compounds, including benzene-1,2-diol, has been shown to cause loss of both strength and modulus of elasticity in concrete [1]. This deterioration is possibly partly the result of expansion [2], and measurements made by the author (to be published in a subsequent article) confirm that exposure to benzene-1,2-diol leads to the expansion of hardened cement paste, possibly as a result of the formation of crystals of at least one of these compounds.

As part of the research, it was necessary to construct concentration profiles of the compounds and other hydration products through cement paste specimens. Analysis using quantitative Rietveld refinement techniques applied to data from powder X-ray diffraction was chosen as a means of doing this. Rietveld refinement requires crystal structure data of all phases in a specimen. The structures of the two compounds have not been determined, and the only data pertaining to their existence in the literature is an infra-red spectrum of a compound formed during an investigation into the formation of stains in vessels

T. D. Dyer (✉)
Concrete Technology Unit, Division of Civil Engineering,
University of Dundee, Dundee DD1 4HN, UK
e-mail: t.d.dyer@dundee.ac.uk

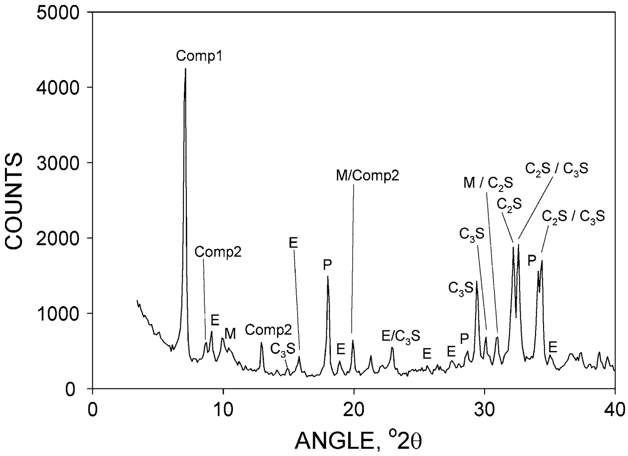

Fig. 1 Powder X-ray diffraction trace obtained from a 7-mm thick slice taken from the surface of a 28-day-old Portland cement paste exposed immediately after mixing to a solution containing 25 g/L of benzene-1,2-diol. *Comp1* Compound 1; *Comp2* Compound 2; *E* ettringite; *P* portlandite; *M* monosulfate; *C_3S* tricalcium silicate; *C_2S* dicalcium silicate

containing tea [3]. Thus, it was desirable to determine the crystal structure of both compounds.

This article characterises these two compounds in terms of their thermal decomposition characteristics, infra-red spectra and crystal structures.

Materials and methods

Preparation

The approach taken to synthesis of the pure compounds was based on an assumption that the complexes were formed in the cement experiments as a result of a reaction between benzene-1,2-diol and calcium hydroxide. Exploratory attempts at synthesis employing calcium hydroxide solutions into which benzene-1,2-diol was added confirmed that this assumption was correct. However, this approach to synthesis presented problems in obtaining the pure compounds in isolation, and ultimately an approach to synthesis involving a reaction between sodium hydroxide and calcium chloride was developed. A range of different combinations of solution concentrations and volumes were initially experimented with, and the preparation methods described below emerged as the most effective.

Compound 1

Compound 1 was prepared by dissolving 5.5 g of benzene-1,2-diol into 420 mL 0.1 M calcium chloride solution. 80 mL of 1 M sodium hydroxide solution was then added. The mixture was sealed in a polyethylene bottle and left for 24 h at 20 °C. The resulting crystals were vacuum filtered and washed on the filter with isopropyl alcohol.

The plate-shaped crystals (Fig. 2) were ground in a McCrone micronising mill using agate cylinders and isopropyl alcohol as the fluid medium. The resulting slurry was dried under an infra-red lamp, whose intensity had been set to produce a temperature of 60 °C at the illuminated surface.

The relative density of the crystals was 1.76, measured by flotation using carbon tetrachloride and bromochloromethane.

Compound 2

Compound 2 was prepared by following the procedure for Compound 1, with the exception that a 0.25 M sodium hydroxide solution was used. The resulting needle-shaped crystals (Fig. 3) had a fibrous texture when examined using the scanning electron microscope.

The relative density of the crystals was 1.49, measured by flotation using chloroform and carbon tetrachloride.

Both compounds were seemingly stable under normal atmospheric conditions, and showed no sign of reaction with atmospheric oxygen or carbon dioxide.

Thermogravimetric analysis

Thermogravimetry (TG) was conducted using a Netsch STA 409 PC instrument. A heating rate of 10 °C/min was employed, whilst nitrogen was passed through the furnace at a rate of 10 mL/min. The exhaust gases from the furnace were passed through a flexible heated pipe maintained at a temperature of 200 °C into a Bruker TGA/IR unit attached to a Bruker Tensor 27 Fourier transform infra-red spectrometer. The spectrometer sequentially measured absorption over a wavenumber range of 4000–700 cm^{-1} at 1-min

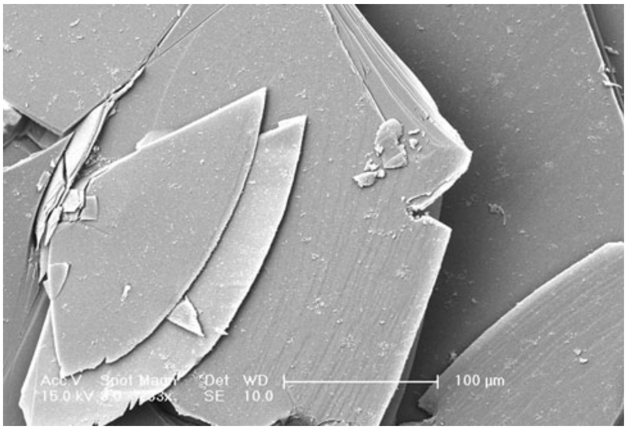

Fig. 2 Scanning electron micrograph showing crystals of Compound 1

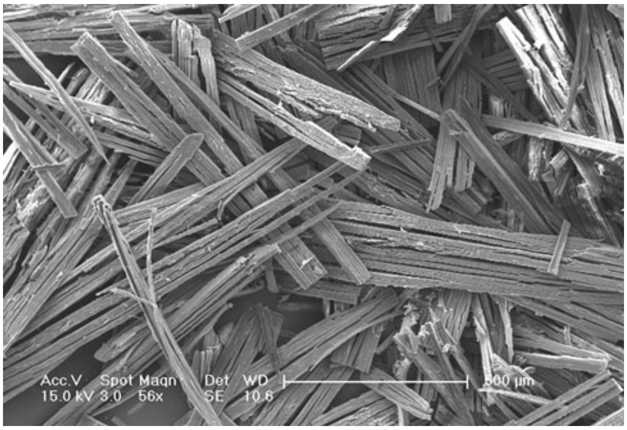

Fig. 3 Scanning electron micrograph showing crystals of Compound 2

intervals. These spectra were collated to produce a composite image of the sequential spectra allowing a ‘map’ with axes of temperature and wavenumber to be constructed.

Infra-red spectrometry

10-mm diameter KBr pellets containing approximately 1% of either compound were prepared under a hydraulic pressure of 750 MPa with evacuation of air from the die chamber during preparation. The pellets were analysed using a Bruker Tensor 27 Fourier transform infra-red spectrometer with spectra collected between 4000 and 400 cm^{-1}.

Powder X-Ray diffraction

The powdered specimens were loaded into specimen holders and analysed using a Philips PW1030 goniometer with a curved graphite single-crystal monochromator and a Cu Kα radiation source. The angular range used was 3 to 70°2θ (Compound 1) and 3 to 60°2θ (Compound 2), in steps of 0.01°2θ at a rate of 0.1°2θ/min. Measurement was conducted at a temperature of 20 °C. In addition, samples containing a 5% corundum internal standard were run under identical conditions to permit correction of any angular error before indexing.

Both compounds’ X-ray powder diffraction patterns were auto-indexed using indexing programs accessed via the Crysfire program [4]. The programs used were DICVOL [5] and TREOR [6]. The best solutions from the possible unit cells identified and the most likely space groups were then established using a combination of manual methods using the CHECKCELL program [7] and the automated Space Group Explorer facility in the FOX program [8].

Structure solution was carried out using a parallel tempering algorithm under the FOX program [8]. Refinement was conducted with the MAUD program [9] using a Marquardt least-squares algorithm. After refinement of both structures, positions of hydrogens attached to carbon atoms on the benzene ring were calculated assuming a bond length of 1.09 Å. Calculation of the positions of hydrogens attached to oxygen atoms (whether as water, hydroxide or hydroxyl groups) was not attempted, although some of these atoms were located during refinement.

The structure solution and refinement procedures followed were specific to the individual compounds and informed by the results of the other techniques. These details are therefore discussed in the Results section.

Results

Thermogravimetric analysis

Compound 1

The TG trace obtained from Compound 1 is shown in Fig. 4, whilst the map obtained from the IR spectra of the exhaust gases is shown in Fig. 5, with the highest intensity spectra from each major event identified on the TG trace also included. The TG trace shows two losses in mass—one occurring at between 200 and 300 °C and one at between 650 and 800 °C. The IR spectra obtained from the exhaust gases indicate that the first loss in mass is the result of the loss of molecules of fully protonated benzene-1,2-diol [10]. The exhaust gases associated with the second loss in mass contain CO, CO_2, possibly H_2O and CH_4 (or higher molecular weight compounds with similar

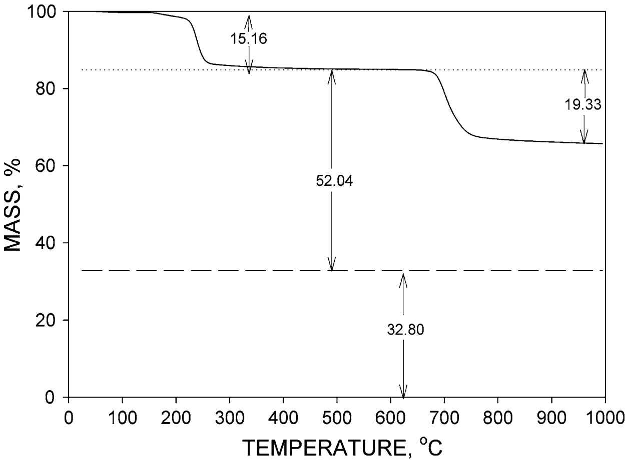

Fig. 4 Thermogravimetry trace from Compound 1. *Dashed line* indicates residual mass after ignition in a muffle furnace at 1000 °C

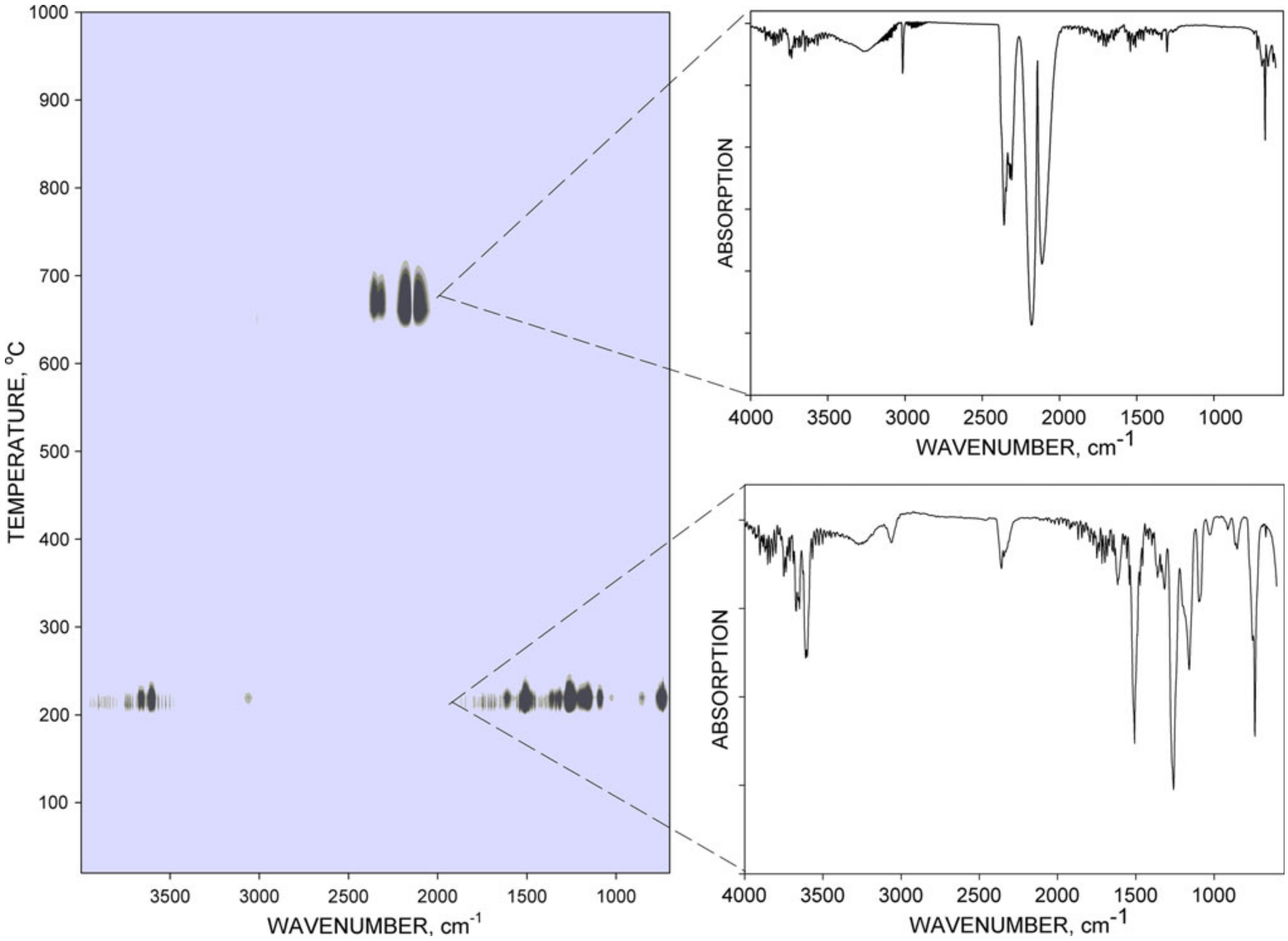

Fig. 5 IR spectra map obtained from exhaust gases evolved during the thermal decomposition in nitrogen of Compound 1 over the range 20–1000 °C, with individual spectra shown from key points in the decomposition process

structural features), which were assumed to be the result of the pyrolysis of the remaining organic constituents.

The residue remaining after thermogravimetric analysis was a black powder. Analysis using X-ray powder diffraction identified the only crystalline component of this residue as calcium oxide, with evidence of a non-crystalline component. Thus, the residue's black colour was assumed to derive from amorphous char from the pyrolysis process. The retention of some of the benzene-1,2-diol up to high temperatures indicates a strong bond between the organic molecule and calcium, which consequently implies that the benzene-1,2-diol is at least partly deprotonated.

Measurement of loss-on-ignition in air in a muffle furnace at 1000 °C yielded a loss in mass of 67.2%. Analysis of the residue confirmed it to be calcium oxide. This residual mass after ignition is marked on Fig. 4.

The release of a fully protonated benzene-1,2-diol molecule during decomposition, the increments in mass loss measured and the requirement for neutrality of charge indicate three possible configurations for the compound.

The first possible configuration is one consisting of one fully protonated benzene-1,2-diol, one benzene-1,2-diolate dianion ($C_6O_2H_4{}^{2-}$) and two calcium ions, giving the formula $[Ca(C_6O_2H_4)]\cdot C_6O_2H_6$. Formulations of this kind containing 'catechol of crystallisation' have been reported previously [11, 12].

The second possible configuration comprises one calcium ion, one benzene-1,2-diolate monoanion ($C_6O_2H_5{}^{-}$) and one hydroxide ion, with the formula $[Ca(C_6O_2H_5)(OH)]$. In this configuration, to satisfy the requirement for the release of a benzene-1,2-diol molecule during decomposition, it would be necessary for the transfer of protons to half of the benzene-1,2-diolate ions in the compound either from other catecholate monoanions or from hydroxide ions. Transfer of protons from a hydroxide ion to a hydroxyphenol molecule has been previously observed during the thermal decomposition of hydroxycalcium phenoxide [13].

The third configuration has the formula $[Ca_2(C_6O_2H_5)(OH)_2](C_6O_2H_6)$.

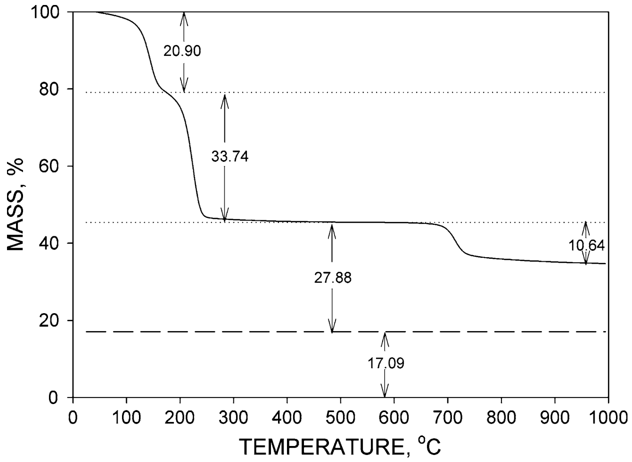

Fig. 6 TG and trace from Compound 2. *Dashed line* indicates residual mass after ignition in a muffle furnace at 1000 °C

Compound 2

Figure 6 shows the TG trace obtained from Compound 2, with the IR-spectra map obtained from the exhaust gases provided in Fig. 7. There are three losses in mass. Two of these events are very similar to those observed in Complex 1, namely, those occurring at between 200 and 300 °C and between 650 and 800 °C, albeit with different magnitudes of mass change. Examination of the spectra map indicates that the events involve the release of the same compounds as Complex 1.

Whilst barely evident from the map, examination of individual spectra obtained from the exhaust gases indicates that the loss in mass observed between 70 and 180 °C is the result of the release of water.

Analysis using X-ray powder diffraction again identified the crystalline component of the residue remaining after TG analysis as calcium oxide with evidence of amorphous char. Loss-on-ignition measurements gave a loss in mass of 82.9%. Analysis of the residue confirmed it to be calcium oxide. The residual mass after ignition is marked on Fig. 6.

From these results, three possible formulae could be proposed: (i) $[Ca(C_6O_2H_4)](Ca_6O_2H_6)\cdot 4H_2O$, (ii) $[Ca(C_6O_2H_5)(OH)](C_6O_2H_6)\cdot 3H_2O$ and (iii) $[Ca(C_6O_2H_5)_2]\cdot 4H_2O$.

Infra-red spectroscopy

Compound 1

Figure 8 shows the FTIR spectrum obtained from Compound 1 over the range 1700–4000 cm^{-1} alongside that of benzene-1,2-diol. Where vibrations belonging to benzene-1,2-diol (as assigned by Öhrström, and Michaud-Soret [14] and Greaves and Griffith [15]) are considered to be present in the spectrum of Compound 1, these are joined by dashed lines.

OH stretches are exhibited by Compound 1 at 3576 and 3514 cm^{-1}, indicating either protonation or partial protonation of the organic molecule, the presence of a hydroxide ion, or both.

The Compound 1 spectrum within the range 900–1700 cm^{-1} (Fig. 9) appears to show the loss of the 1364 cm^{-1} OH bending mode band, but the retention of the OH bend at 1186 cm^{-1} (shifted to 1205 cm^{-1}). This is characteristic of the benzene-1,2-diolate monoanion [15], indicating partial deprotonation. Considering the possible formulae identified in the previous section, it must be concluded that the compound contains a hydroxide ion.

It was assumed that the band at 1320 cm^{-1} results from a shift of one of the three bands which occur between 1300 and 1200 cm^{-1} in benzene-1,2-diol. Such a feature is characteristic of co-ordination between metals and benzene-1,2-diolate ions [16]. There is some debate with regards how these bands should be assigned, but it is assumed here that they are to some extent associated with C–O stretching.

Absorption at 588 cm^{-1} in Fig. 10 can be attributed to Ca–O stretching, since M–O stretches in most metal alkoxides are usually exhibited below 600 cm^{-1} [17]. M–O–H bending (resulting from co-ordination to a hydroxide ion) normally produces absorption below 1200 cm^{-1}, allowing possible assignment to either the 924 (Fig. 9) or 866 cm^{-1} bands (Fig. 10). Both bands possibly also contain contributions from bands from benzene-1,2-diol, such as that at 849 cm^{-1}. Assignments are discussed further in the following section.

Compound 2

Compound 2 also displays OH stretches (Fig. 11), this time at 3543, but with other absorption features around this frequency. Resolution of the bands in the infra-red spectrum for Compound 2 is poorer than for Compound 1, although it is clear from Fig. 12 that the general form of the spectra within the range 1700–900 cm^{-1} remains very similar to that of benzene-1,2-diol. The presence of water in the compound should see the presence of bands relating to the H–O–H bend. These bands are probably present as a shoulder of the band at 1609 cm^{-1}. It is also worth noting that the magnitude of the bands assigned to OH bending in benzene-1,2-diol is significantly diminished in the calcium compound. It is likely that the band at 1364 cm^{-1} is wholly absent, whilst the 1186 cm^{-1} band is very weak. As for Compound 1, the shift of a ring vibration from outside the 1300–1200 cm^{-1} range to 1306 cm^{-1} is tentatively proposed, indicating co-ordination between calcium and a benzene-1,2-diolate ion.

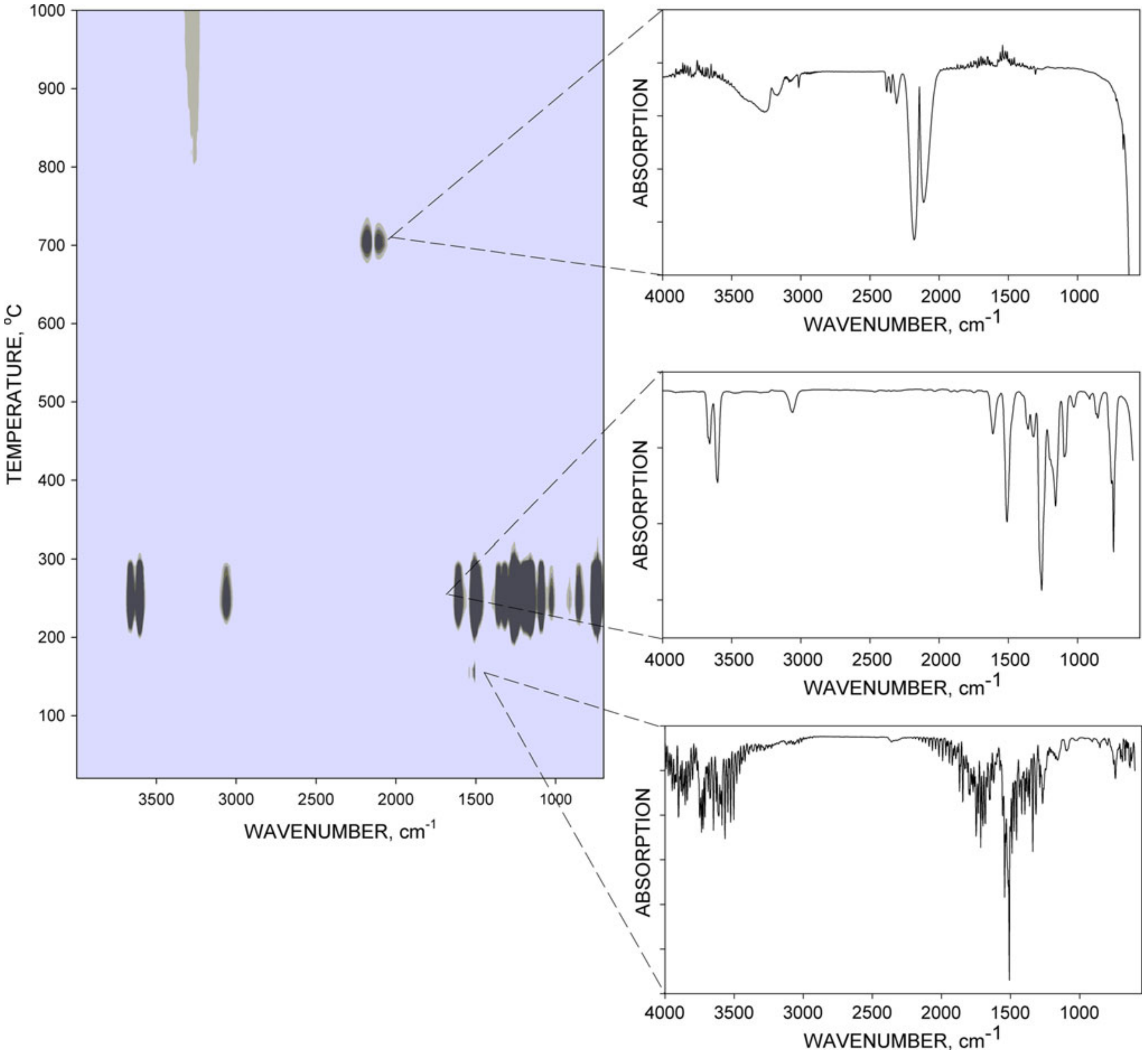

Fig. 7 IR spectra map obtained from exhaust gases evolved during the thermal decomposition in nitrogen of Compound 2 over the range 20–1000 °C, with individual spectra shown from key points in the decomposition process

The main differences between the Compound 2 and benzene-1,2-diol spectra appear within the 900–400 cm^{-1} range where there are new bands at 591 cm^{-1} and probably 859 cm^{-1} (Fig. 13). As for Compound 1, the lower frequency band was attributed to a Ca–O stretch. The 859 cm^{-1} band was tentatively assigned to a rocking mode of H_2O co-ordinated to Ca.

It was considered possible that the presence of benzene-1,2-diol at two different states of deprotonation (as in the formula $[Ca(C_6O_2H_5)(OH)](C_6O_2H_6)\cdot 3H_2O$) would, at least in part, explain the broad and poorly defined bands in the spectrum. This was of only minor significance in deducing the crystal structure since, minus the hydrogen atoms, all three possible configurations contained the same constituents. Discussion of the compound composition continues in the following section.

Powder X-ray diffraction

Powder X-ray diffraction traces obtained from Compounds 1 and 2 are shown in Figs. 14 and 15, respectively. The patterns match the peaks observed in the cement paste specimen in Fig. 1.

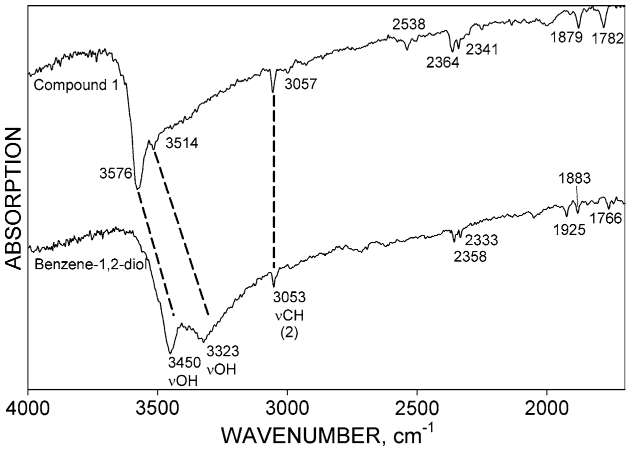

Fig. 8 FTIR trace of Compound 1 in the wavenumber range of 1700–4000 cm^{-1} alongside that of benzene-1,2-diol. The *dashed lines* represent proposed assignments for Complex 1 corresponding to those assigned by Öhrström and Michaud-Soret [14] and Greaves and Griffith [15] for benzene-1,2-diol

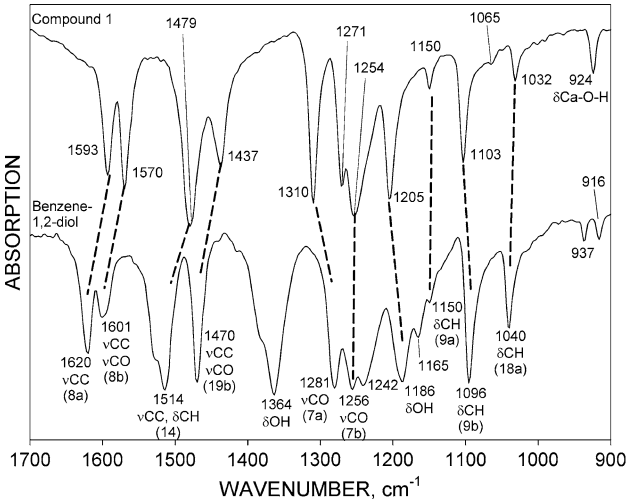

Fig. 9 FTIR trace of Complex 1 in the wavenumber range of 900–1700 cm^{-1} alongside that of benzene-1,2-diol. The *dashed lines* represent proposed assignments for Complex 1 corresponding to those assigned by Öhrström and Michaud-Soret [14] and Greaves and Griffith [15] for benzene-1,2-diol

Indexing

In the case of Compound 1, this was an orthorhombic unit cell with space group Pbca. For Compound 2, the best unit cell was also orthorhombic, with the most likely space group being Pnn2. Unit cells and space groups for both compounds were consistent with asymmetric units containing a single formula unit. From the unit cell dimensions and density measurements, the formula $[Ca(C_6O_2H_5)(OH)]$—(benzene-1,2-diolato(1-))hydroxidocalcium(II)—was identified as being the most probable.

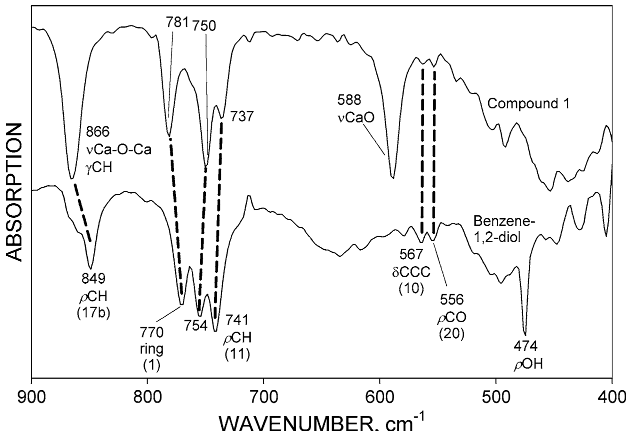

Fig. 10 FTIR trace of Complex 1 in the wavenumber range of 400–900 cm^{-1} alongside that of benzene-1,2-diol. The *dashed lines* represent proposed assignments for Complex 1 corresponding to those assigned by Öhrström and Michaud-Soret [14] and Greaves and Griffith [15] for benzene-1,2-diol

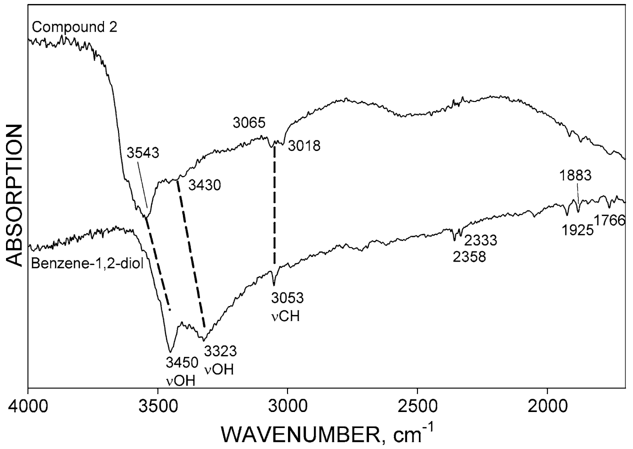

Fig. 11 FTIR trace of Compound 2 in the wavenumber range of 1700–4000 cm^{-1} alongside that of benzene-1,2-diol. The *dashed lines* represent proposed assignments for Complex 1 corresponding to those assigned by Öhrström and Michaud-Soret [14] and Greaves and Griffith [15] for benzene-1,2-diol

Structure solution

In the case of Compound 1, the unit cell was populated with one calcium atom, one oxygen atom (representing the hydroxide ion) and a benzene-1,2-diol molecule [18], minus the hydrogen atoms, which was treated as a rigid body. FOX's 'smart' temperature schedule was employed for running the algorithm with default settings for parallel tempering. 20 parallel tempering runs were performed, each comprising ten million trials. All of the runs yielded a very similar structure. The lowest R_{wp} value obtained was 0.1147, and the structure from this run was used for subsequent refinement.

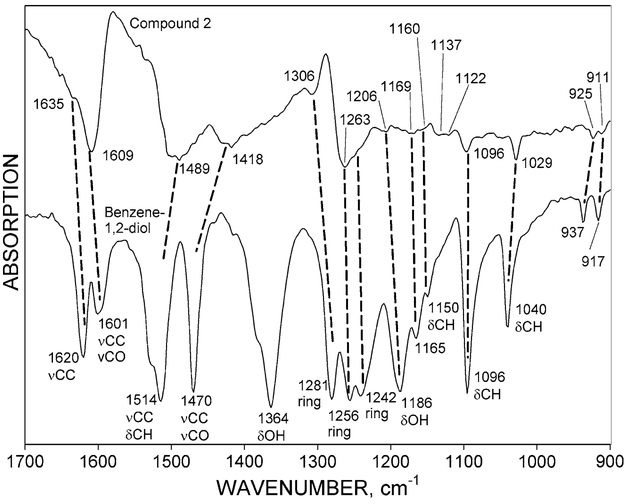

Fig. 12 FTIR trace of Complex 2 in the wavenumber range of 900–1700 cm^{-1} alongside that of benzene-1,2-diol. The *dashed lines* represent proposed assignments for Complex 1 corresponding to those assigned by Öhrström and Michaud-Soret [14] and Greaves and Griffith [15] for benzene-1,2-diol

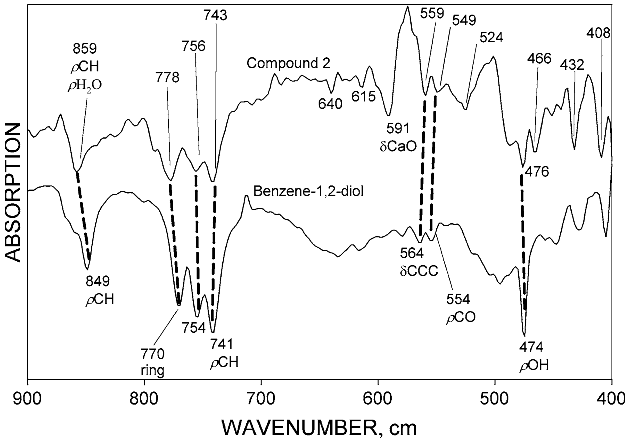

Fig. 13 FTIR trace of Complex 2 in the wavenumber range of 400–900 cm^{-1} alongside that of benzene-1,2-diol. The *dashed lines* represent proposed assignments for Complex 1 corresponding to those assigned by Öhrström and Michaud-Soret [14] and Greaves and Griffith [15] for benzene-1,2-diol

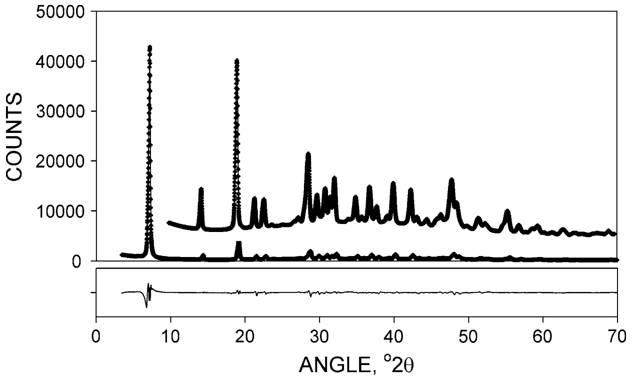

Fig. 14 Rietveld plot obtained after structure solution and refinement of powder X-ray diffraction data obtained from Compound 1

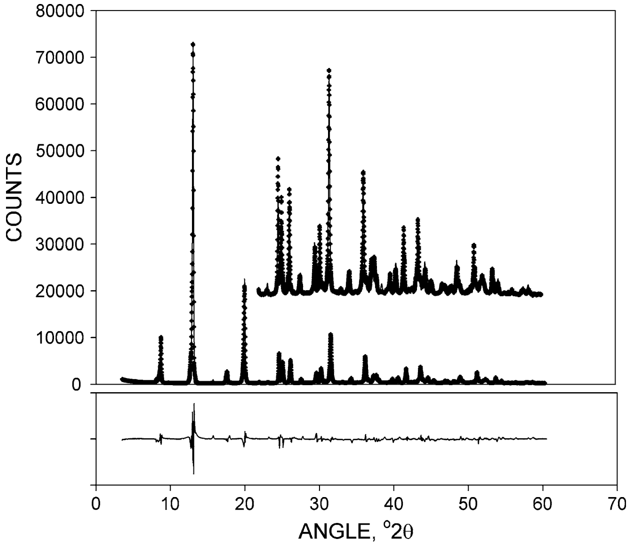

Fig. 15 Rietveld plot obtained after structure solution and refinement of powder X-ray diffraction data obtained from Compound 2

The unit cell for Compound 2 was populated with two calcium atoms, four oxygen atoms (representing either water or hydroxide) and two rigid body benzene-1,2-diol molecules without hydrogen atoms. The same settings as for Compound 1 were used for parallel tempering. Again, the structure selected for refinement was that with the lowest R_{wp} value (0.1848).

Refinement

For Compound 1, 50 parameters were refined using all 381 reflections within the range measured. From the refinement of the structure of Compound 1, a final R_{wp} value of 0.078 was obtained (Fig. 14). The relatively high value was believed to be the result of poor fitting of some peak profile shapes. This was attributed to partial delamination of crystal layers and attempts were made to model such defects by various means. However, this was not successful in resolving the problem. Refinement of isotropic temperature displacement factors yielded some negative and high magnitude values, leading to the conclusion that modelling of background at the higher angular range was not adequate. Attempts to improve this did not resolve the problem. Both of the remaining hydrogen atoms were located through examination of difference Fourier maps and refinement repeated with geometrical restraints.

55 Parameters were refined for Compound 2 using all 322 reflections within the measured range. An R_{wp} value of 0.110 was obtained after refinement (Fig. 15). Again, examination of peak shapes indicated possible partial

delamination, but modelling of this effect was not effective in improving fits to peaks. Similar problems with refining temperature displacement factors were encountered, and it must be concluded that the quality of the X-ray data obtained using the equipment available may not have been sufficient to allow refinement towards meaningful values in the case of both compounds. Examination of difference Fourier maps located one of the remaining hydrogen atoms, and refinement was repeated with this atom included in the unit cell.

Discussion

Compound 1

The unit cell and atomic parameters of Compound 1 are provided in Table 1, and the structure is shown in Fig. 16. The structure consists of layers of calcium ions each co-ordinated to eight oxygens. The calcium ions are sandwiched between, and bidentally chelated by, benzene-1,2-diolate monoanions located either side of this layer. The rings of these ions are aligned in parallel to the *c*-axis. The calcium ions are arranged in a similar, albeit distorted, hexagonal configuration to that of $Ca(OH)_2$ [19]. Moreover, the benzene-1,2-diolate oxygens are located in similar locations to the oxygens of the hydroxide ions in the same compound in a trinucleating bridging co-ordination with calcium ions. The hydroxide ion in the structure also acts as a bridge between pairs of calcium ions, leading to the likely conclusion that the 866 cm^{-1} band in the IR spectrum is a Ca–O–Ca stretch–stretch interaction [20], and the 924 cm^{-1} band can be attributed to the Ca–O–H bending mode.

Table 1 Crystal structure data for Compound 1

Formula	$[Ca(C_6O_2H_5)(OH)]$
Name	(Benzene-1,2-diolato(1-))hydroxidocalcium(II)
Crystal system	Orthorhombic
Space group	Pbca
a	6.506(6)
b	7.792(5)
c	24.729(4)

	x	*y*	*z*
Ca and hydroxide			
Ca	0.2420	0.3616	0.0000
OH1	0.9709	0.7079	0.4480
HO1	0.0198	0.2432	0.0868
Benzene-1,2-diolate			
C1	0.0739	0.6668	0.0957
C2	0.1207	0.6044	0.1470
C3	0.0575	0.6941	0.1927
C4	0.9476	0.8461	0.1871
C5	0.9008	0.9084	0.1359
C6	0.9640	0.8187	0.0902
O2	0.1207	0.5770	0.0486
O3	0.9132	0.8931	0.0407
H1[a]	0.7068	0.4852	0.3487
H2[a]	0.5941	0.6453	0.2671
H3[a]	0.3980	0.9164	0.2771
H4[a]	0.3147	1.0275	0.3685
H5	0.5395	0.1869	0.5092

[a] Calculated positions

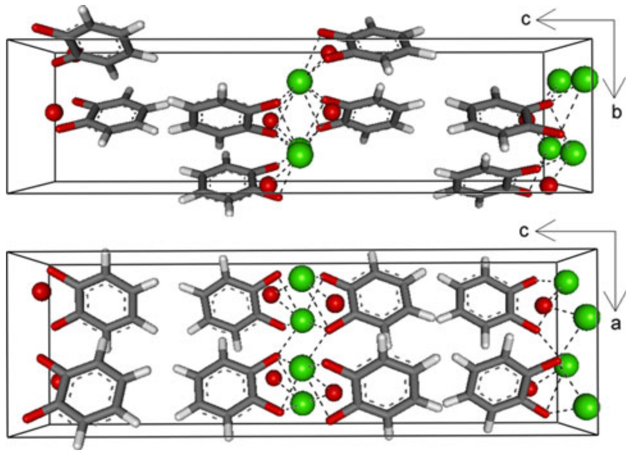

Fig. 16 Structure of Compound 1 viewed along (i) the *a*-axis and (ii) the *b*-axis. *Dotted lines* denote co-ordination to the Ca ion

The co-ordination polyhedron formed approximates to No. 128 in the system devised by Britton and Dunitz [21]—a distorted square antiprism. These polyhedra are joined in pairs by triangular faces and joined by their edges to adjacent polyhedra pairs (Fig. 17). The polyhedra pairs are arranged in a herringbone configuration. Atom O2 is the deprotonated catecholate oxygen.

It is interesting to note that the hydrogen on the hydroxide ion points away from the other oxygen atoms, and is thus not involved in hydrogen bonding. This feature is also seen in $Ca(OH)_2$, and the absence of hydrogen bonding produces a high frequency OH-stretch vibration (3650 cm^{-1}) on its IR spectra [22]. This explains the occurrence of OH-stretch vibrations at relatively high wavenumber ranges in Compound 1.

Table 2 provides distances between selected atoms in the structure. The bond length of the only hydrogen bond in the structure is also provided in the table. This is notably short, which is likely to be the result of the charge-assisted nature of this bond.

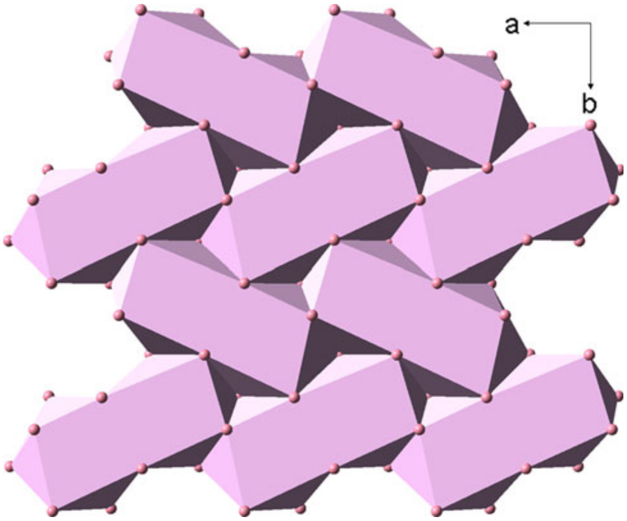

Fig. 17 Co-ordination polyhedra in Compound 1, viewed along the *c*-axis

From the characterisation of Compound 1, it can be assumed that its thermal decomposition in the absence of oxygen can be written in one of two ways, depending on the manner in which protons are transferred to catecholate ions:

Between 200 and 300 °C:

$$4[\mathrm{Ca(C_6O_2H_5)(OH)}] \rightarrow \left[\mathrm{Ca_4(C_6O_2H_5)_3(OH)_3O}\right] + \mathrm{C_6O_2H_6}$$

Between 650 and 800 °C:

$$\left[\mathrm{Ca_4(C_6O_2H_5)_3(OH)_3O}\right] \rightarrow 4\mathrm{CaO} + \text{gases} + \text{char.}$$

Alternatively, the two decomposition events are:

$$4[\mathrm{Ca(C_6O_2H_5)(OH)}] \rightarrow \left[\mathrm{Ca_4(C_6O_2H_4)(C_6O_2H_5)_2(OH)_4}\right] + \mathrm{C_6O_2H_6},$$

$$\left[\mathrm{Ca_4(C_6O_2H_4)(C_6O_2H_5)_2(OH)_4}\right] \rightarrow 4\mathrm{CaO} + \text{gases} + \text{char.}$$

The precise mechanisms of pyrolysis in the final decomposition stage and the full range of resulting products are not determinable from the results of this study.

Table 2 Selected interatomic distances in the Compound 1 structure

		Distance, Å
Ca	Ca	3.691/3.819/3.899
Ca	O1	2.238/2.333
Ca	O2	2.024/2.751/2.793
Ca	O3	2.431/2.452/2.470
O3(–H5)	···O1	2.457
H5	···O1	1.646

Compound 2

Unit cell and atomic parameters for Compound 2 are given in Table 3. Its structure is shown in Fig. 18. Again, the structure contains a layer of calcium ions, although the layer is shared with oxygens from either water molecules or hydroxide ions. This layer, again, lies between layers of benzene-1,2-diol molecules or benzene-1,2-diolate ions, although these are aligned at an angle of approximately 45$^{\mathrm{o}}$ to the *c*-axis. Again, the calcium ion is co-ordinated to eight oxygens, with the phenolic molecules bidentally chelating the metal. The co-ordination polyhedron formed approximates to a distorted square anti-prism. The polyhedra do not share any faces or edges with their neighbours (Fig. 19).

Distances between selected atoms in the structure are given in Table 4. Ca–O distances in the co-ordination polyhedron indicate a closer proximity of oxygen O4 to the calcium ion, distinguishing it from oxygens O1 to O3. This was interpreted as meaning that O4 was present as a hydroxide ion, making the second possible configuration identified by thermal analysis the most likely. However, the co-ordination of all oxygens in the unit cell to the calcium ion means that the compound's formula should be written as $[\mathrm{Ca(C_6O_2H_5)(C_6O_2H_6)(H_2O)_3(OH)}]$ and is thus named triaqua(benzene-1,2-diol)(benzene-1,2-diolato(1-))hydroxidocalcium(II). From this formula and the located hydrogen atom, the most likely hydrogen bond configurations were deduced and are presented in Table 4. Thus, the co-ordination polyhedra are hydrogen bonded to each other along the *b*-axis as shown in Fig. 19.

The thermal decomposition of the compound in the absence of oxygen is:

Between 70 and 180 °C:

$$\left[\mathrm{Ca(C_6O_2H_5)(C_6O_2H_6)(H_2O)_3(OH)}\right] \rightarrow [\mathrm{Ca(C_6O_2H_5)(C_6O_2H_6)(OH)}] + 3\mathrm{H_2O}.$$

Between 200 and 300 °C:

$$[\mathrm{Ca(C_6O_2H_5)(C_6O_2H_6)(OH)}] \rightarrow [\mathrm{Ca(C_6O_2H_5)(OH)}] + \mathrm{C_6O_2H_6}$$

immediately followed by the same decomposition reactions undergone by Compound 1 within this temperature range and pyrolysis between 650 and 800 °C.

Conclusions

Two compounds formed between hydrated Portland cement and benzene-1,2-diol have been synthesised and characterised. It is anticipated that both the thermal analysis data obtained, and crystal structures deduced, in this article can now be used to quantify these phases in cement

Table 3 Crystal structure data for Compound 2

Formula	$[Ca(C_6O_2H_5)(C_6O_2H_6)(H_2O)_3(OH)]$		
Name	Triaqua(benzene-1,2-diol)(benzene-1,2-diolato(1-))hydroxidocalcium(II)		
Crystal system	Orthorhombic		
Space group	Pnn2		
a, Å	7.240(9)		
b, Å	10.118(0)		
c, Å	20.471(4)		
	x	*y*	*z*
Ca, water and hydroxide			
Ca1	0.1805	0.7694	0.0000
OW1	0.4568	0.7421	0.0821
OW2	0.1959	0.5180	0.4971
OW3	0.8098	−0.0097	0.5019
OH4	0.2583	0.6748	0.9001
Benzene-1,2-diol			
C1	0.3876	0.6693	0.6126
C2	0.2815	0.5987	0.6583
C3	0.1678	0.6669	0.7027
C4	0.1604	0.8055	0.7013
C5	0.2665	0.8760	0.6556
C6	0.3800	0.8078	0.6112
O5	0.4848	0.5943	0.5743
O6	0.5101	0.9116	0.5775
H1[a]	0.6933	0.5452	0.8189
H2[a]	0.5621	0.6917	0.7325
H3[a]	0.6206	0.9345	0.7360
H4[a]	0.8099	1.0310	0.8260
Benzene-1,2-diolate			
C7	0.3252	0.7942	0.3713
C8	0.2186	0.8487	0.3205
C9	0.1448	0.7662	0.2718
C10	0.1777	0.6294	0.2738
C11	0.2843	0.5751	0.3245
C12	0.3580	0.6576	0.3732
O7	0.3931	0.8530	0.4290
O8	0.4383	0.6172	0.4168
H5[a]	0.2873	0.4910	0.6594
H6[a]	0.0855	0.6121	0.7381
H7[a]	0.0723	0.8585	0.7356
H8[a]	0.2607	0.9837	0.6545
H9	0.4717	0.1339	0.4267

[a] Calculated positions

and concrete exposed to benzene-1,2-diol in experiments through TG or Rietveld refinement techniques applied to powder X-ray diffraction data.

It should be stressed that the characteristics established in this article do not provide any further evidence of whether these compounds are responsible in any way for the deterioration of concrete in contact with benzene-1,2-diol. It is possible that deterioration is, in part, the result of expansion of the cement matrix due to the precipitation of these compounds. However, it is recognised that there is little value in comparing volumes of reactants and products as a means of implicating a phase formed in hardened cement in causing swelling, and that volumetric changes are more commonly the result of crystallisation pressure

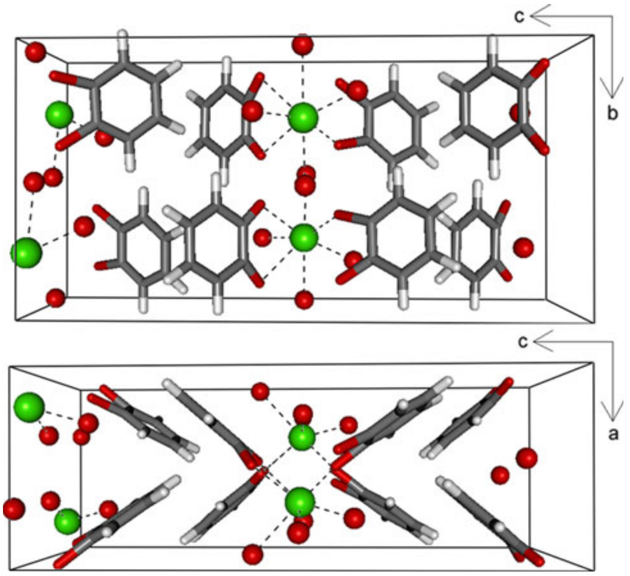

Fig. 18 Structure of Compound 1 viewed along (i) the *a*-axis and (ii) the *b*-axis. *Dashed lines* denote co-ordination to the Ca ion

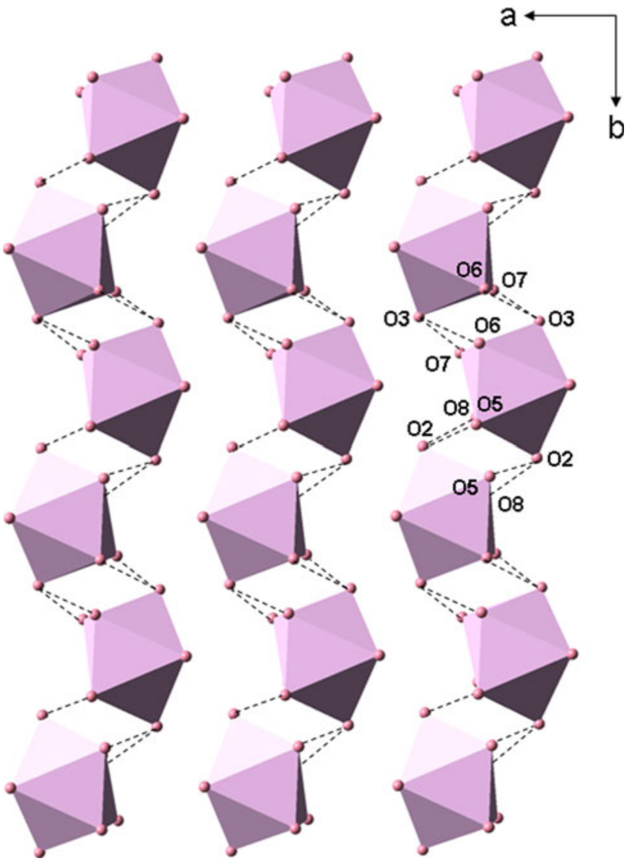

Fig. 19 Co-ordination polyhedra in Compound 2, viewed along the *c*-axis. *Dashed lines* denote O···O pairs involved in hydrogen bonding between co-ordination polyhedra

Table 4 Selected interatomic distances in the Compound 2 structure

		Distance, Å			Distance, Å
Ca	Ca	5.364	OW2	···O5	2.741
Ca	O1	2.634	OW2	···O8	2.613
Ca	O2	2.678	OW3	···O4	2.704
Ca	O3	2.797	OW3	···O7	2.634
Ca	O4	2.334	O6	···O3	2.966
Ca	O5	2.502	O7(-H9)	···O4	2.733
Ca	O6	2.726	H9	···O4	1.806
Ca	O7	2.832			
Ca	O8	2.708			

[23]. Nonetheless, the results are useful, since the ability to quantify these phases permits correlations between their formation and both expansion and deterioration to be examined.

Location of the remaining hydrogen atoms in the tri-aqua(benzene-1,2-diol)(benzene-1,2-diolato(1-))hydroxido-calcium(II) unit cell may be possible via neutron diffraction methods.

Characterisation of the product of partial thermal decomposition of both compounds (either $[Ca_4(C_6O_2H_5)_3(OH)_3O]$ or $[Ca_4(C_6O_2H_4)(C_6O_2H_5)_2(OH)_4]$) and further study of the final pyrolysis process has not been undertaken by this author, since neither is sufficiently relevant to the research motivating the activities reported in this article. Nonetheless, investigation may prove valuable in other fields.

References

1. Živica V (2006) Constr Build Mater 20:634
2. Živica V, Bajza A (2001) Constr Build Mater 15:331
3. Yamada K, Abe T, Tanizawa Y (2007) Food Chem 103:8
4. Shirley R (1999) The CRYSFIRE system for automatic powder indexing: user's manual. Lattice Press, Guildford
5. Boultif A, Louer D (2004) J Appl Crystallogr 37:724
6. Werner P-E, Eriksson L, Westdahl M (1985) J Appl Crystallogr 18:367
7. Laugier J, Bochu B (2011) LMGP-suite suite of programs for the interpretation of X-ray experiments, by, ENSP/Laboratoire des Matériaux et du Génie Physique, Saint Martin d'Hères, France. http://www.inpg.fr/LMGP and http://www.ccp14.ac.uk/tutorial/lmgp/
8. Favre-Nicolin V, Cerny R (2002) J Appl Crystallogr 35:734
9. Lutterotti L, Matthies S, Wenk H-R, Schultz AJ, Richardson J (1997) J Appl Phys 81:594
10. Wilson HW (1974) Spectrochim Acta A 30(1974):2141
11. Rosenheim A, Mong H (1925) Z Anorg Allg Chem 148:25
12. Griffith WP, Pumphrey CA, Rainey T-A (1986) J Chem Soc Dalton Trans 6:1125
13. Schlosberg RH, Scouten CG (1988) Energy Fuel 2:582
14. Öhrström L, Michaud-Soret I (1999) J Phys Chem A 103:256

15. Greaves SJ, Griffith WP (1991) Spectrochim Acta A 47:133
16. Michaud-Soret I, Andersson KK, Que L (1995) Biochemistry-US 34:5504
17. Nakamoto K (2009) Infrared and Raman Spectra of inorganic and co-ordination compounds—part B, 6th edn. Wiley, Hoboken
18. Brown CJ (1966) Acta Crystallogr 21:170
19. Busing WR, Levy HA (1957) J Chem Phys 26:563
20. Wing RM, Callahan KP (1969) Inorg Chem 8:871
21. Britton D, Dunitz JD (1973) Acta Crystallogr A29:362
22. Hamilton WC, Ibers JA (1968) Hydrogen bonding in solids. Benjamin, New York
23. Scherer GW (2004) Cem Concr Res 34:1613